

Probing CP-violating Higgs contributions in $\gamma\gamma \rightarrow f\bar{f}$ through fermion polarization

Rohini M. Godbole*

Center for High Energy Physics, IISc, Bangalore 560 012, India

Sabine Kraml†

Theory Division, Department of Physics, CERN, CH-1211 Geneva 23, Switzerland

Saurabh D. Rindani‡

Physical Research Laboratory, Navrangapura, Ahmedabad 380 009, India

Ritesh K. Singh§

Laboratoire de Physique Théorique, 91405 Orsay Cedex, France

We discuss the use of fermion polarization for studying neutral Higgs bosons at a photon collider. To this aim we construct polarization asymmetries which can isolate the contribution of a Higgs boson ϕ in $\gamma\gamma \rightarrow f\bar{f}$, $f = \tau/t$, from that of the QED continuum. This can help in getting information on the $\gamma\gamma\phi$ coupling in case ϕ is a CP eigenstate. We also construct CP-violating asymmetries which can probe CP mixing in case ϕ has indeterminate CP. Furthermore, we take the MSSM with CP violation as an example to demonstrate the potential of these asymmetries in a numerical analysis. We find that these asymmetries are sensitive to the presence of a Higgs boson as well as its CP properties over a wide range of MSSM parameters. In particular, the method suggested can cover the region where a light Higgs boson may have been missed by LEP due to CP violation in the Higgs sector, and may be missed as well at the LHC.

PACS numbers: 14.80.Cp, 14.60.Fg, 12.60.Jv

I. INTRODUCTION

The Higgs boson is the only particle of the Standard Model (SM) to have eluded experimental discovery so far. The discovery of the Higgs boson and the subsequent study of electroweak symmetry breaking is one of the prime aims of all the current and next generation colliders [1]. Electroweak precision measurements indicate, in the SM, the existence of a Higgs boson lighter than 204 GeV at 95% C.L. [2]. A Higgs boson with SM couplings lighter than 114.4 GeV is ruled out by direct searches at LEP [3]. Thus one expects to find the SM Higgs boson with a mass in this range. In models with an extended (and possibly CP-violating) Higgs sector, the couplings of electroweak vector bosons to the lightest Higgs can be suppressed [4]. In such a case direct searches allow the existence of a Higgs boson much lighter than 114.4 GeV [5].

The Large Hadron Collider (LHC), scheduled to go in operation in 2007, is expected [6] to be capable of searching for the SM Higgs boson in the entire mass range expected theoretically and still allowed experimentally. The International Linear Collider (ILC) [7], currently in planning, is expected to be capable of profiling the Higgs boson very accurately, again for the entire mass range mentioned above. Determination of the CP properties of the spin-0 particle, which we hope will be discovered and studied at the LHC and the ILC, is an important part of this project of profiling the Higgs boson, see e.g. [8]. The

Higgs couplings with a pair of electroweak gauge bosons ($V = W/Z$) and those with a pair of heavy fermions ($f = t/\tau$) are the ones that prove the most useful in this context. These couplings, for a neutral Higgs boson ϕ , which may or may not be a CP eigenstate, can be written as

$$\phi f\bar{f} : \frac{-ig m_f}{2 M_W} (v_f + ia_f \gamma_5) \quad (1)$$

$$\phi VV : \frac{ig M_V^2}{M_W} \left(A_V g_{\mu\nu} + B_V \frac{p_\mu p_\nu}{M_Z^2} + i C_V \epsilon_{\mu\nu\rho\sigma} \frac{p^\rho q^\sigma}{M_Z^2} \right) \quad (2)$$

where $p = P_{V_1} + P_{V_2}$, $q = P_{V_1} - P_{V_2}$ and P_{V_1} , P_{V_2} are the four momenta of the two massive vector bosons. In the SM, $v_f = A_V = 1$ and $a_f = B_V = C_V = 0$. At the LHC, the $t\bar{t}$ final state produced in the decay of an inclusively produced Higgs can provide knowledge of the CP nature of the $t\bar{t}\phi$ coupling through spin-spin correlations [9] whereas $t\bar{t}\phi$ production can allow a determination of v_f and a_f [10]. It should also be possible to exploit the ϕZZ coupling via $\phi \rightarrow ZZ \rightarrow l^+l^-l'^+l'^-$ [11], and the vector boson fusion mode [12]. At the ILC [7], a rather clean determination of the CP of the Higgs boson should be possible using the Higgsstrahlung process [13]. Angular correlations of the decay products of the ϕ , in particular $\phi \rightarrow f\bar{f}$, may be used effectively at an e^+e^- collider to distinguish between $v_f = 1, a_f = 0$ and $v_f = 0, a_f = 1$ as well as to get information on CP mixing [14]. A remark is in order here. The different methods which exploit the $VV\phi$ coupling test the terms with tensor structure $g_{\mu\nu}$ and $\epsilon_{\mu\nu\rho\sigma}$ in Eq. (2); actually in most cases the CP-even part $\propto g_{\mu\nu}$ is projected out since in most CP violating (CPV) extensions of the SM one has $A_V \gg B_V, C_V$. The $f\bar{f}\phi$ coupling, on the other hand, allows equal sensitivity

*Electronic address: rohini@cts.iisc.ernet.in

†Electronic address: Sabine.Kraml@cern.ch

‡Electronic address: saurabh@prl.res.in

§Electronic address: Ritesh.Singh@th.u-psud.fr

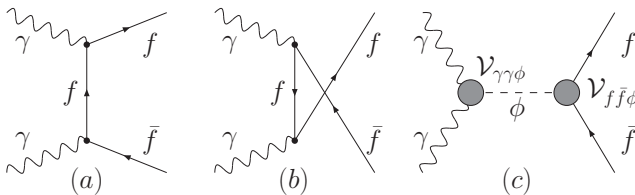


FIG. 1: Feynman diagrams contributing to $\gamma\gamma \rightarrow f\bar{f}$ production.

to the CP-even and CP-odd parts. At both colliders, the LHC and the ILC, the determination of the CP quantum number of the Higgs boson seems feasible, while determination of CP mixing seems difficult; the best chance for the latter being offered by the exploitation of the $f\bar{f}\phi$ coupling [15].

A more sensitive laboratory for studying the CP properties of a neutral Higgs boson is the photon collider option [16] of the ILC. At a photon collider, the Higgs boson is produced resonantly in the s -channel and thus one will be able to produce it copiously even if the $\gamma\gamma\phi$ coupling is small. In presence of CP violation (CPV), the CP-even and CP-odd components of the Higgs couple to photons with comparable strength. A study of the production rates with linearly- and circularly-polarized photons can help determine the CP quantum numbers if conserved, as well as the CP mixing phases in the case of CP violation. Angular distributions of decay products (VV , $b\bar{b}$) of the produced ϕ along with measurements of $\Gamma(\phi \rightarrow b\bar{b})$, $\Gamma(\phi \rightarrow \gamma\gamma)$ may also allow the determination of a CP-mixing phase [17]; the $\phi \rightarrow t\bar{t}$ decay can also be used [18, 19] if it is kinematically allowed. While a complete reconstruction of couplings would require both circularly and linearly polarized photons [18], substantial information can already be obtained using circularly polarized photons alone [19]. Polarization of the final state fermions, which are pair produced, can be a probe of CP violation in the production process [18, 19, 20]. Among SM fermions, the polarization can be measured only for t -quarks and tau-leptons. The t -quark decays before it hadronizes and hence the polarization information gets reflected in the angular distributions of decay products, whereas for the τ lepton one can extract polarization information by looking at the energy distribution of pions [21, 22]. For a Higgs mass larger than $2m_t$, top polarization is the best probe of the Higgs interaction. However, for a CP-violating light Higgs boson, which could have escaped detection at LEP, the decay into $t\bar{t}$ is not possible. In this case the $\tau^+\tau^-$ final state might provide a useful probe. We therefore study the contribution of a light Higgs boson to τ production via $\gamma\gamma \rightarrow \phi \rightarrow \tau^+\tau^-$ and that of heavier Higgs bosons to τ production via $\gamma\gamma \rightarrow \phi \rightarrow t\bar{t}$. Higgs contribution to τ polarization has also been studied recently for the LHC [23], for a photon collider [24] and for an e^+e^- linear collider [25] in the context of resonant CP violation in the MSSM. The effect of neutral Higgs boson exchange in $\gamma\gamma \rightarrow t\bar{t}$ has been addressed in Ref. [18, 19, 26], in

terms of various correlations and asymmetries for a photon collider.

In this paper, we investigate the possibility of using tau/top polarization to get information on the $\phi f\bar{f}$ and $\phi\gamma\gamma$ couplings, as well as to probe possible CP violation in them in a generic scenario. First, we formulate the method in a model-independent way. We then apply it in a numerical analysis to the minimal supersymmetric standard model with CP violation (CPV-MSSM). The neutral Higgs sector of the CPV-MSSM has been studied in detail theoretically [27], and constraints from LEP are available [5]. In this work, we study τ/t polarization in the CPX scenario [28] over regions of the CPV-MSSM parameter space that are allowed by the current data, and assess the feasibility of using it to probe the Higgs contribution to $f\bar{f}$ production. In the numerical analysis, we use `CPsuperH` [29] and `FeynHiggs 2.1` [30] for calculating the masses, the decay widths and the relevant couplings of the Higgs bosons.

The rest of the paper is organized as follows. In section II, we describe fermion pair production at a $\gamma\gamma$ collider in a model-independent way. Section III deals with polarization observables as potential probes of the Higgs contribution and its CP structure. Numerical results within the CPV-MSSM are presented in section IV, and in section V we present our conclusions.

II. FERMION PAIR PRODUCTION IN $\gamma\gamma$ COLLISION

At a photon collider, the production of a fermion pair involves the $\gamma f\bar{f}$, $\gamma\gamma\phi$ and $\phi f\bar{f}$ vertices as shown in Fig. 1. We take the $\gamma f\bar{f}$ vertex to be the standard QED one, while the vertices involving Higgs bosons are taken to be the most general allowed. The model independent vertex for Higgs interactions with fermions is given in Eq. (1) and with a pair of photons, allowing for CP violation, can be written as :

$$\mathcal{V}_{\gamma\gamma\phi}^{\mu\nu} = \frac{-i\sqrt{s}\alpha}{4\pi} \left[A_\gamma(s) \left(g^{\mu\nu} - \frac{2}{s} k_1^\nu k_2^\mu \right) - B_\gamma(s) \frac{2}{s} \epsilon^{\mu\nu\alpha\beta} k_{1\alpha} k_{2\beta} \right]. \quad (3)$$

Here k_1 and k_2 are the four-momenta of the colliding photons. The helicity amplitudes for fermion pair production in the s - and the t/u -channels can be obtained from those given in [18, 19] :

$$M_\phi(\lambda_1, \lambda_2; \lambda_f, \lambda_{\bar{f}}) = \frac{-ig\alpha m_f}{8\pi M_W} \frac{s}{s - m_\phi^2 + im_\phi\Gamma_\phi} [A_\gamma(s) + i\lambda_1 B_\gamma(s)] [\lambda_f \beta v_f - ia_f] \delta_{\lambda_1, \lambda_2} \delta_{\lambda_f, \lambda_{\bar{f}}}, \quad (4)$$

$$M_{QED}(\lambda_1, \lambda_2; \lambda_f, \lambda_{\bar{f}}) = \frac{-i4\pi\alpha Q^2}{1 - \beta^2 \cos^2 \theta_f} \left[\frac{4m_f}{\sqrt{s}} (\lambda_1 + \lambda_f \beta) \delta_{\lambda_1, \lambda_2} \delta_{\lambda_f, \lambda_{\bar{f}}} - \frac{4m_f}{\sqrt{s}} \lambda_f \beta \sin^2 \theta_f \delta_{\lambda_1, -\lambda_2} \delta_{\lambda_f, \lambda_{\bar{f}}} - 2\beta (\cos \theta_f + \lambda_1 \lambda_f) \sin \theta_f \delta_{\lambda_1, -\lambda_2} \delta_{\lambda_f, -\lambda_{\bar{f}}} \right]. \quad (5)$$

TABLE I: Combinations of form factors v_f , a_f , A_γ and B_γ that occur in the helicity amplitudes of Eqs. (4) and (5).

Combination	Alias	CP	Combination	Alias	CP
$v_f \Re(A_\gamma)$	x_1	even	$v_f \Im(A_\gamma)$	x_2	even
$v_f \Re(B_\gamma)$	y_1	odd	$v_f \Im(B_\gamma)$	y_2	odd
$a_f \Re(A_\gamma)$	y_3	odd	$a_f \Im(A_\gamma)$	y_4	odd
$a_f \Re(B_\gamma)$	x_3	even	$a_f \Im(B_\gamma)$	x_4	even

The form factors A_γ and B_γ are complex whereas v_f, a_f can be taken to be real without loss of generality. The non-standard vertices given by Eqs. (1) and (3) involve four independent form factors: v_f , a_f , A_γ , B_γ . In the MSSM with CPV, these form factors are functions of various model parameters: $\tan\beta$; m_{H^\pm} ; $(|\mu|, \Phi_\mu)$; $(|A_{\tilde{f}}|, \Phi_{\tilde{f}})$; $(|M_i|, \Phi_i)$, $i = 1, 2, 3$; $m_{\tilde{q}, \tilde{l}}$; etc., where $(|x|, \Phi_x)$ denotes $x = |x|e^{i\Phi_x}$.

The helicity amplitudes of Eqs. (4) and (5) involve only certain combinations of the form factors which are listed in Table I. Only five of these eight combinations are independent, the other three can be obtained by interrelations such as $x_1 x_3 = y_1 y_3$, etc. In all the extensions of the SM, A_γ and B_γ are generated at the one-loop level. Simultaneous existence of v_f and a_f , or A_γ and B_γ violates CP, i.e. non-vanishing values of y_i , ($i = 1, \dots, 4$) imply CP violation. Even in case of CP invariance, where only the x_i 's are non-zero, the Higgs contribution can alter the polarization of the fermions f from that predicted by pure QED. CP violation, giving rise to non-zero y_i 's, gives an additional contribution to the fermion polarization.

It should be noted that the Higgs-mediated diagram contributes only when the helicities of the colliding photons are equal. The helicities of f and \bar{f} are also equal in this case. The QED contribution for this helicity combination is proportional to the fermion mass. Both these facts indicate that one should choose equal photon helicities to enhance the effect of the Higgs mediated diagram. The contribution with opposite helicities of photons comes from QED diagrams alone and it is large as compared to that of equal photon helicities for $\sqrt{s} \gg 4m_f$. Thus with unpolarized photons the net contribution from Higgs exchange will be relatively small. Hence one expects poor sensitivity to the Higgs contribution with unpolarized initial state photons.

Among the vertices contributing to fermion-pair production, the standard $\gamma f \bar{f}$ vertex conserves chirality, while the $\phi f \bar{f}$ vertex mixes different chiralities. Owing to the finite mass m_f of the fermion, there is a chirality-mixing contribution even for the pure QED diagrams (Figs. 1a,b). The presence of the Higgs boson exchange, Fig. 1c, provides an additional, polarization dependent, spatially isotropic, chirality-mixing contribution. The property of spatial isotropy is unique to Higgs exchange contribution, in contrast to other means of chirality mixing, such as the finite mass effect. With unpolarized initial-state photons, the QED as well as a CP-conserving Higgs contribution lead to unpolarized fermions in the final state; CP violation in the Higgs sector leads to a net, though very small, fermion polarization. With

polarized initial-state photons, already pure QED leads to a finite polarization. The additional chirality mixing from the Higgs exchange causes a change in this polarization in both the CP-conserving and the CP-violating case. It is thus possible to construct observables relating initial-state photon and final-state τ/t polarizations which probe the Higgs couplings as well as possible CP violation in the Higgs sector.

III. FERMION POLARIZATION IN $\gamma\gamma$ COLLISION

At a $\gamma\gamma$ collider, Compton back-scattering of a laser from e^-/e^+ is used to produce high-energy photons[31]. The energy spectrum of the back-scattered photons depends upon the polarizations of the e^-/e^+ beams and the laser as shown in Fig. 2. This figure shows the distribution of the reduced invariant mass of the $\gamma\gamma$ system $z = \sqrt{\omega_1 \omega_2}/E_b$, where $\omega_{1,2}$ are the energies of the two colliding photons in the lab frame, for a laser energy ω_0 corresponding to

$$x_c = \frac{4E_b \omega_0}{m_e^2} = 4.8. \quad (6)$$

The spectrum is peaked in the high energy region for opposite polarizations of the electron and laser beams. Further, most of these high-energy photons have a large degree of polarization. By choosing appropriate polarizations for the e^-/e^+ and laser beams, one can thus obtain a peaked and highly polarized spectrum for the colliding photons. We shall use this fact when constructing various observables with τ polarization.

The polarization of fermions is defined as the fractional surplus of positive helicity fermions over negative helicity ones, i.e.

$$P_f^{ij} = \frac{N_+^{ij} - N_-^{ij}}{N_+^{ij} + N_-^{ij}}, \quad (7)$$

where the superscript ij stands for the polarizations of the parent e^-, e^+ beams of the ILC (with P_f^{++} meaning 100% right polarized electrons and 100% right polarized positrons); N_+ and N_- stands for the number of fermions with positive and negative helicities, respectively. Analogously, \bar{P}_f^{ij} is the polarization of the anti-fermion. Due to the left-chiral nature of the W -boson interaction, the positively and negatively polarized f 's lead to different distributions of the decay products. For τ 's, by looking at the net energy distribution of decay π one can get information on its polarization [21]. On the other hand, for t -quarks, it is the energy distribution of b -quarks or the angular distribution of decay leptons.

The various N_\pm^{ij} , and hence P_f^{ij} , with different polarizations of initial-state photons are related to each other via discrete symmetry transformations, such as C, P and CP, if these symmetries are respected by the underlying dynamics. Thus any deviation from these relations can be a probe of the violation of the corresponding discrete symmetry.

For unpolarized initial-state photons the polarization, P_f^U , is zero for the QED diagrams (Figs. 1a,b). Even in

TABLE II: Polarization observables and interactions and combinations that they can probe.

Observables	Interactions probed	Combinations probed
P_f^U	P/CP violating	y_i 's
$\delta P_f^+ = P_f^{++} - (P_f^{++})^{QED}$	Chirality-mixing	x_i 's, y_i 's
$\delta P_f^- = P_f^{--} - (P_f^{--})^{QED}$	Chirality-mixing	x_i 's, y_i 's
$\delta P_f^{CP} = P_f^{++} + P_f^{--}$	P/CP violating	y_i 's

the presence of a CP-conserving Higgs P_f^U is zero. This is because the left chiral and the right chiral components of fermions couple to the Higgs boson with equal strength. Thus the net polarization of the fermions, if any, will signal CP violation in the Higgs sector. In general it is a signal of P violation, but in the process under consideration f couples only to self-conjugate neutral particles, γ and ϕ . Hence $P_f^U \neq 0$ is also a signal of CP violation. We note that P_f^U is a pure but a poor probe of CPV.

For polarized initial state photons, QED predicts a non-zero value of P_f and this prediction is modified by the presence of the Higgs exchange diagram. The deviation from the QED prediction is a probe of the Higgs contribution and hence its couplings. We define

$$\delta P_f^+ = P_f^{++} - (P_f^{++})^{QED}, \quad (8)$$

$$\delta P_f^- = P_f^{--} - (P_f^{--})^{QED}. \quad (9)$$

Such a deviation does not have any definite P or CP property, thus it can be non-zero even when the Higgs boson is a CP eigenstate. This allows us to detect the presence of a Higgs over a large range of x_i 's and y_i 's (and hence a large range of model parameters, as we will see later) by measuring the fermion (t/τ) polarization. We choose equal polarization of e^+ and e^- beams so as to have equal helicities for the colliding photons; this enhances the chirality-mixing Higgs contribution as discussed in the previous section, c.f. Eqs. (4) and (5).

In QED, the polarization of f flips its sign if we change the signs of the polarizations of the initial state photons (actually those of the electron and positron of the parent collider), i.e. $P_f^{++} = -P_f^{--}$. This is due to P invariance of QED. Also, due to the self-conjugate nature of the neutral particles involved, we have $P_f^{ii} = \bar{P}_f^{ii}$. In CP-violating models, however, we expect $P_f^{++} + P_f^{--} \neq 0$. Although it is a probe of P violation in general, it will be a probe of CP violation in our process. In Table II we list all the observables and their potentials. The definitions in Eqs. (8) and (9), along with the fact that $(P_f^{++})^{QED} = -(P_f^{--})^{QED}$, implies

$$\delta P_f^{CP} = \delta P_f^+ + \delta P_f^-. \quad (10)$$

For polarized photons we therefore have two independent observables, δP_f^- and δP_f^{CP} . These can be sizable over a large range of, for instance, MSSM parameters and hence can be used to probe the Higgs interactions. As we have already mentioned, the expected polarization P_f^U for unpolarized photons is very small. In Fig. 3 we show, as an example, expected values of δP_f^\pm and δP_f^{CP} as functions of E_b for a Higgs mass of 54 GeV and $v_\tau = 2.0$,

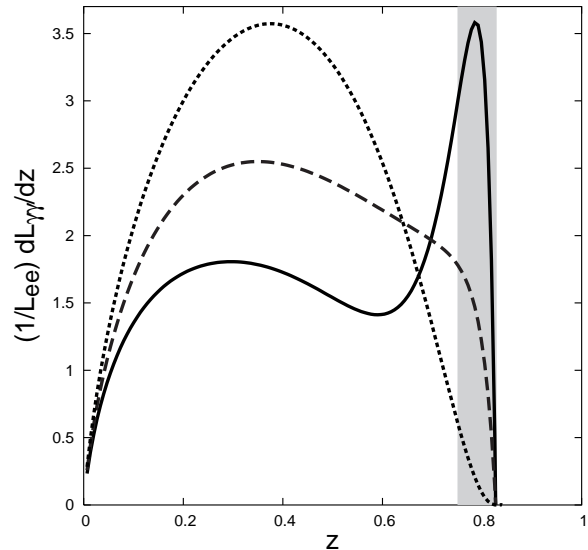


FIG. 2: Luminosity distribution plotted against z (which is related to the $\gamma\gamma$ invariant mass $W = 2\sqrt{\omega_1\omega_2}$ via $z = W/(2E_b)$) for $x_c = 4.8$. The solid line corresponds to $\lambda_e\lambda_l = -1$, the short-dashed line is for $\lambda_e\lambda_l = 1$, and the long-dashed one for $\lambda_e\lambda_l = 0$. The conversion distance is taken to be zero. The grey patch highlights the region $0.75 < z < 0.83$.

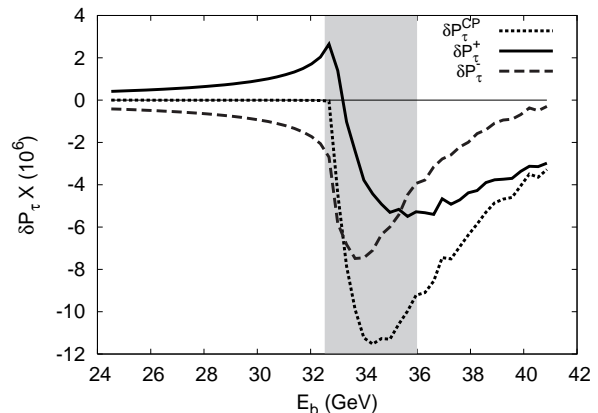


FIG. 3: Variation of δP_f^+ , δP_f^- and δP_f^{CP} as a function of E_b for a Higgs boson of mass 54 GeV. For a value of E_b in the grey patch, the mass of the Higgs boson matches with the $\gamma\gamma$ invariant mass in the grey band shown in Fig. 2.

$a_\tau = -2.3$, $A_\gamma = -0.76 + 0.032i$, $B_\gamma = -0.13 + 0.039i$. The peak in δP occurs when the Higgs mass matches with the $\gamma\gamma$ invariant mass corresponding to the peak of photon spectrum in Fig. 2. By adjusting the beam energy E_b , we can thus maximize the sensitivity of the polarization observables defined above. Details of the selection criteria for E_b for a scan over the parameters of a model are discussed in Section V.

IV. THE CPV-MSSM HIGGS SECTOR

We choose the MSSM as an example for demonstrating the potential of the observables constructed in the previous section to isolate the Higgs boson contribution

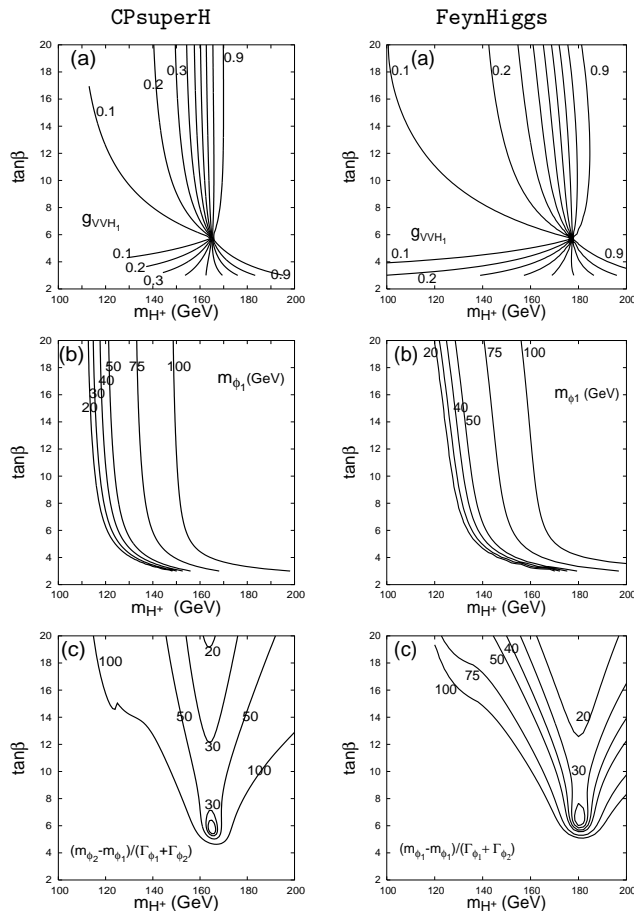


FIG. 4: CPX scenario: contours of (a) A_V (see Eq.(2)) for $V = W, Z$, (b) m_{ϕ_1} and (c) $(m_{\phi_2} - m_{\phi_1})/(\Gamma_{\phi_1} + \Gamma_{\phi_2})$ computed with **CPsuperH** as well as **FeynHiggs**.

TABLE III: List of MSSM parameters for the CPX scenario used as input for the programs **CPsuperH** and **FeynHiggs**.

MSSM param.	Value	MSSM param.	Value
$\tan\beta$	3–40 (for scan)	m_{H^+}	150–500 GeV (for scan)
μ	2 TeV, $\Phi_\mu = 0$	M_1, M_2	200 GeV, $\Phi_{1,2} = 0$
M_3	1 TeV, $\Phi_3 = 90^\circ$	$m_{\tilde{q}, \tilde{l}}$	500 GeV
$A_{t,b}$	1 TeV, $\Phi_{t,b} = 90^\circ$	A_τ	500 GeV, $\Phi_\tau = 90^\circ$

and to probe the CP properties of its couplings. In the CP-conserving MSSM, there exist three neutral Higgs bosons: the CP-even h, H and the CP-odd A . CP-violating phases of the MSSM parameters such as the higgsino mass parameter μ , gaugino masses M_i ($i = 1, 2, 3$) and trilinear couplings A_f ($f = t, b, \tau$), can induce CP violation in the Higgs sector via loops. This allows Higgs states with different CP to mix; the three mass eigenstates hence do not have definite CP. These states are denoted by ϕ_1, ϕ_2 and ϕ_3 with their masses in increasing order. For the numerical analysis, we choose the so-called CPX [28] scenario with parameters as listed in Table III. In this scenario, one can have large CP-violating effects in the Higgs sector depending upon the size of the phases of the trilinear couplings $A_{t,b,\tau}$. Due to this large CP violation, the coupling of the lightest state ϕ_1 to vector

bosons can go down drastically for some values of m_{H^+} and $\tan\beta$, see Fig. 4(a). This results in highly suppressed production rates for the lightest Higgs boson; the lower bound on the mass of such a Higgs boson from direct searches at LEP can be as low as 10–50 GeV [5]. We take into account all three neutral Higgs bosons in the calculation of the fermion polarization by adding their s -channel diagrams. This may, however, not be valid in some regions of the CPV-MSSM parameter space where the Higgs masses become nearly degenerate, i.e. the mass difference of two Higgs bosons is smaller than sum of their widths and hence mixing between these states is resonantly enhanced. In this case one should do a coupled channel analyze [26, 32] of the degenerate states. Fortunately, in the region of parameter space we consider, the mass differences are always much larger than the sum of the decay widths, see Fig. 4(c). Thus our analysis is complementary to that of Refs. [26, 32].

V. NUMERICAL RESULTS

At a photon collider, the center of mass energy of the colliding photons is not fixed but has a wide spectrum. The shape of this spectrum depends upon the polarizations of the laser and the e^+/e^- beams of the parent collider. For the numerical calculation of cross sections, we use the ideal Compton back-scattered spectrum [31] with polarizations of the electron beam and the laser chosen such that one obtains the hard spectrum in Fig. 2. The parent electron beam energy, E_b , can be chosen to maximize the deviation from the QED prediction, cf. Fig. 3. Our observables are maximized when the Higgs mass matches the value of the $\gamma\gamma$ invariant mass at the peak of the polarized photon spectrum. This happens for $E_b = (m_{\phi_i}/2)/z$, where z (the scaled $\gamma\gamma$ invariant mass, $z = \sqrt{\omega_1\omega_2}/E_b$) takes a value between 0.75 to 0.83 for $x_c = 4.8$. This corresponds to the case where the scaled Higgs mass, $m_{\phi_i}/2E_b$, lies in the grey band of Fig. 2.

We can therefore pursue two different strategies for choosing E_b :

1. Parameterizing the relationship between m_{ϕ_i} and E_b in terms of z_0 as $E_b = (m_{\phi_i}/2)/z_0$, we choose an optimal value of z_0 , say $z_0 = 0.80$, for each point in the scan such that δP is maximized. This gives a very good estimate of the ultimate potential of the particular observable used in adaptation. We call this the “peak E_b ” choice.
2. Fixing E_b such that the relevant Higgs mass (m_{ϕ_1} for $\tau^+\tau^-$ and m_{ϕ_2,ϕ_3} for $t\bar{t}$ production) matches approximately with the $\gamma\gamma$ invariant mass corresponding to z values within the peak of the photon spectrum (the grey band in Fig. 2). Though this choice does not exploit the observable optimally, it is closer to what will be done in a realistic experiment. We call this the “fixed E_b ” choice.

In the case of τ polarization, due to the small values of m_τ and Γ_{ϕ_1} , the absolute values of the polarization observables are $\lesssim 10^{-5}$. These can be enhanced by

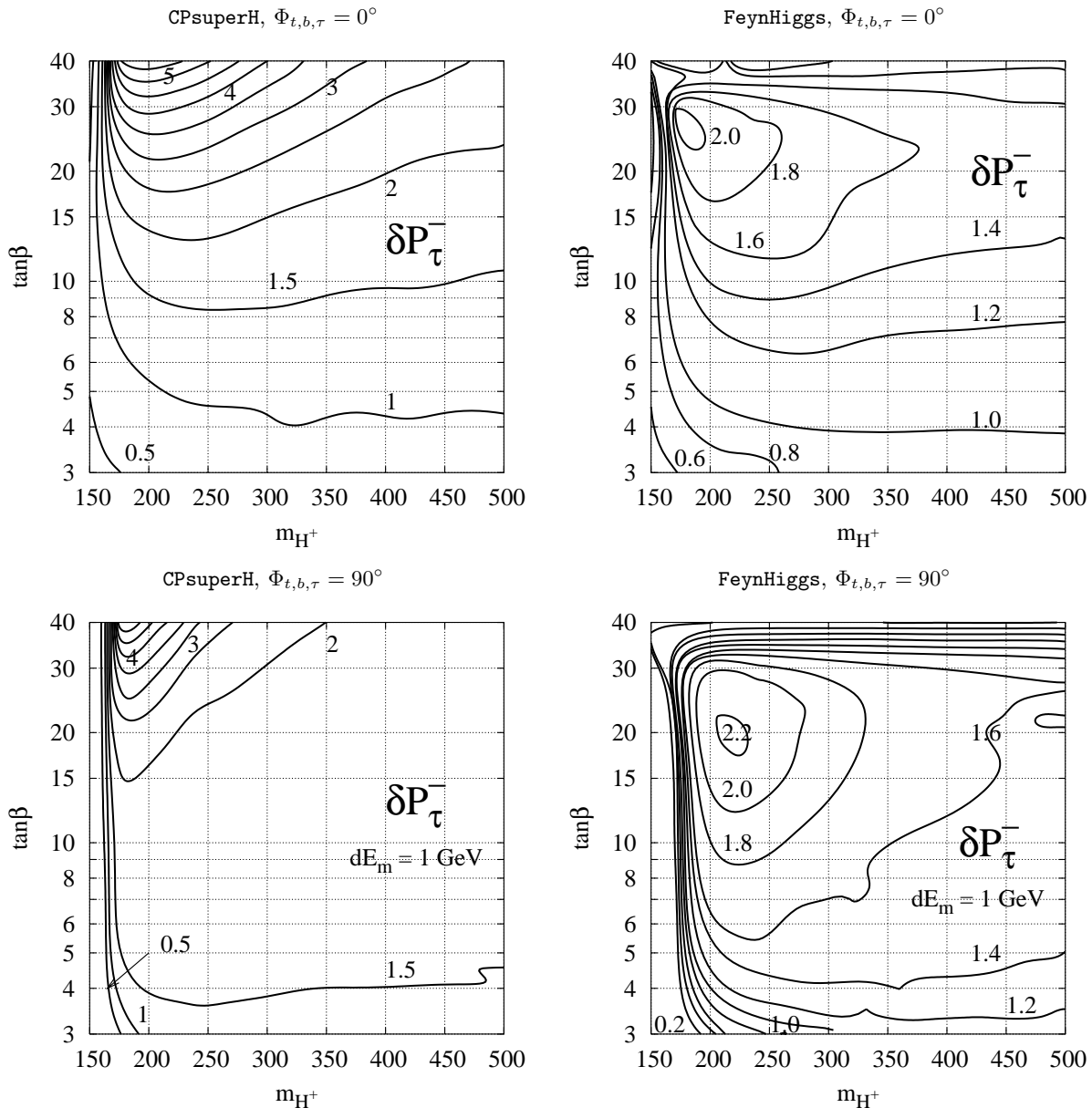


FIG. 5: Contours of constant δP_τ^- in units of 10^{-2} in the $(\tan\beta - m_{H^+})$ plane for the CPX scenario with $\Phi_{t,b,\tau} = 0^\circ$ (top panels) and $\Phi_{t,b,\tau} = 90^\circ$ (bottom panels) for the “peak E_b ” choice with $dE_m = 1$ GeV. The left panels show the results obtained with **CPsuperH**, the rights panels those obtained with **FeynHiggs**.

putting a cut on the invariant mass of the $\tau^+\tau^-$ pair to select the ones coming from ϕ_1 decay [33] :

$$|m_{\tau\tau} - m_{\phi_1}| \leq \max(dE_m, 5 \Gamma_{\phi_1}), \quad (11)$$

where dE_m is the minimum resolution of $m_{\tau\tau}$ reconstruction. We use $dE_m = 1$ GeV for purposes of illustration in this paper. For the case of top production such a cut is not necessary.

In the following, we perform a scan over the MSSM parameters as given in Table III and calculate the τ and t polarization observables for both the peak and the fixed E_b choices using both **CPsuperH** and **FeynHiggs** for calculating the Higgs masses, couplings, and widths. The statistical fluctuation in the value of the fermion polar-

ization is given by

$$\Delta P_f = \frac{\sqrt{1 - P_f^2}}{\sqrt{N_+ + N_-}}. \quad (12)$$

The typical value of ΔP_f for an integrated luminosity of 100 fb^{-1} is about 0.003 for a total rate of 1 pb. The typical τ -pair production rate with the above cut is about 1–10 pb over the $(\tan\beta - m_{H^+})$ plane. τ decays into hadronic channels reduce the useful cross section and hence cause this error to increase. As a conservative measure we take $\delta P_\tau \geq 0.01$ in order to be measurable. The $t\bar{t}$ production rate, on the other hand, is less than 1 pb for the energies considered, and it can be as low as 8 fb with the “peak E_b ” choice in some regions of the $(\tan\beta - m_{H^+})$ plane. Thus the statistical error in the polarization mea-

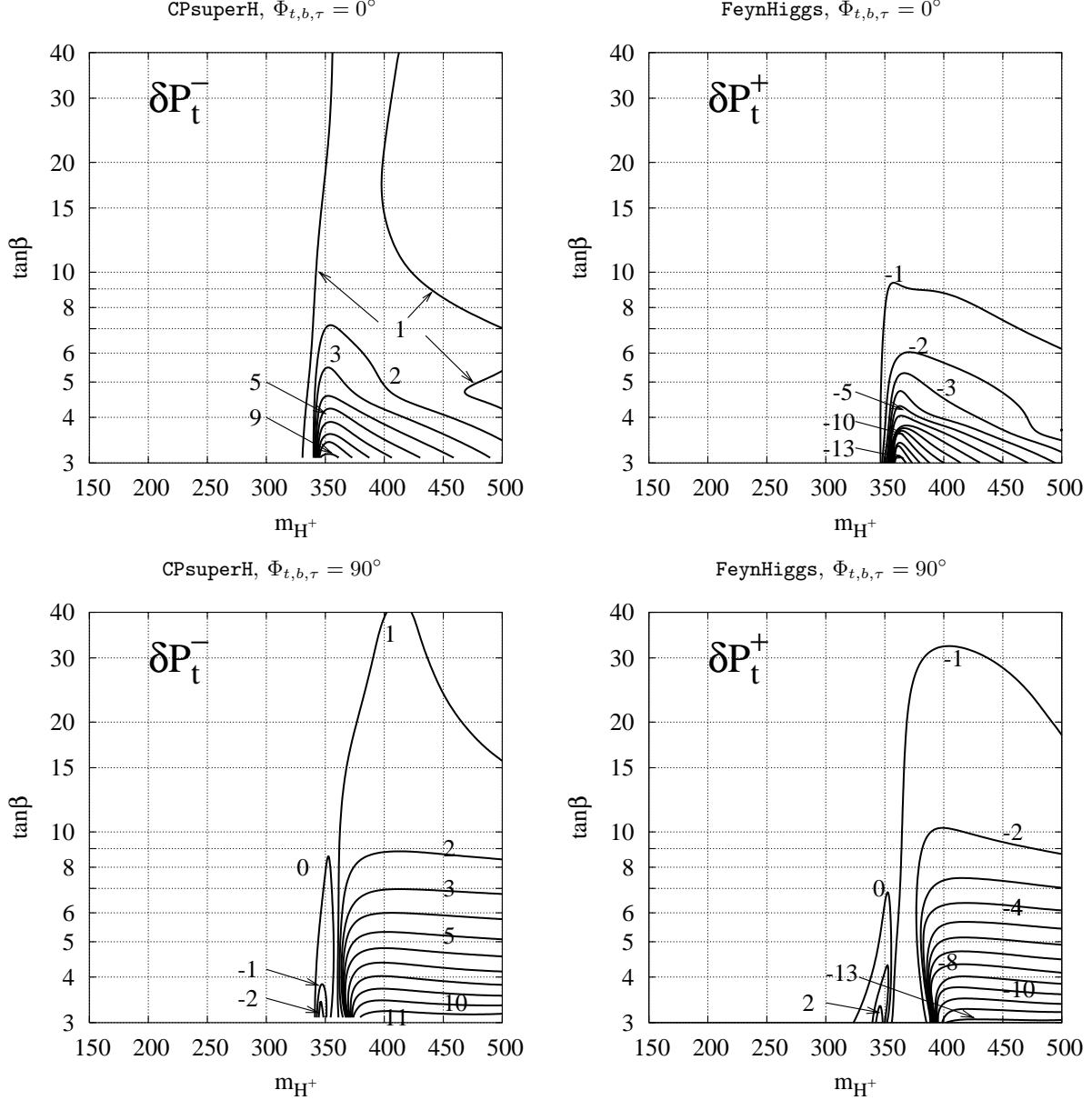


FIG. 6: Contours of constant δP_t^\pm in units of 10^{-2} in the $(\tan\beta - m_{H^+})$ plane for the CPX scenario with $\Phi_{t,b,\tau} = 0^\circ$ (top panels) and $\Phi_{t,b,\tau} = 90^\circ$ (bottom panels) for the “peak E_b ” choice. The left panels show the results for δP_t^- obtained with CPsuperH and the right panels those for δP_t^+ obtained with FeynHiggs, see text.

surement goes up and the sensitivity goes down in this case, even if the polarization asymmetry is large.

A. Peak E_b scan

We first discuss the case of τ -pair production through ϕ_1 exchange for the “peak E_b ” choice. Figure 5 shows contours of constant δP_τ^- as obtained with CPsuperH and FeynHiggs in the $(\tan\beta - m_{H^+})$ plane for $\Phi_{t,b,\tau} = 0^\circ$ and $\Phi_{t,b,\tau} = 90^\circ$. For each point in the scan, the beam energy is set to $E_b = m_{\phi_1}/(2z_0)$ to maximize δP_τ^\pm . In the CP-conserving case, $\Phi_{t,b,\tau} = 0^\circ$, δP_τ^- should be measurable for $\tan\beta \geq 4$ and $m_{H^+} \geq 200$ GeV; smaller values of m_{H^+} require somewhat higher $\tan\beta$ to achieve

$\delta P_\tau^- \geq 0.01$. In the case of maximal CPV phases, $\Phi_{t,b,\tau} = 90^\circ$, $\delta P_\tau^- > 0.01$ holds over practically the entire parameter range, including the region where a very light Higgs boson may have been missed at LEP2 [5]. Such a light CPV Higgs boson will also be difficult to discover at the LHC [34]. The process $\gamma\gamma \rightarrow \tau^+\tau^-$ may hence offer a unique possibility for this case. While δP_τ^- covers a large part of the parameter space, the CP-odd observable $\delta P_\tau^{\text{CP}}$ is very small, $\delta P_\tau^{\text{CP}} \sim 10^{-5}$, and hence below the limit of measurability even if the CPV phases are maximal. This means in turn that $\delta P_\tau^+ \approx -\delta P_\tau^-$. It is also worth noting that the size of the observable is rather sensitive to the value of dE_m : increasing for instance dE_m from 1 GeV to 2 GeV, δP_τ^- goes down by about a factor of 2 over most of the parameter space in Fig. 5.

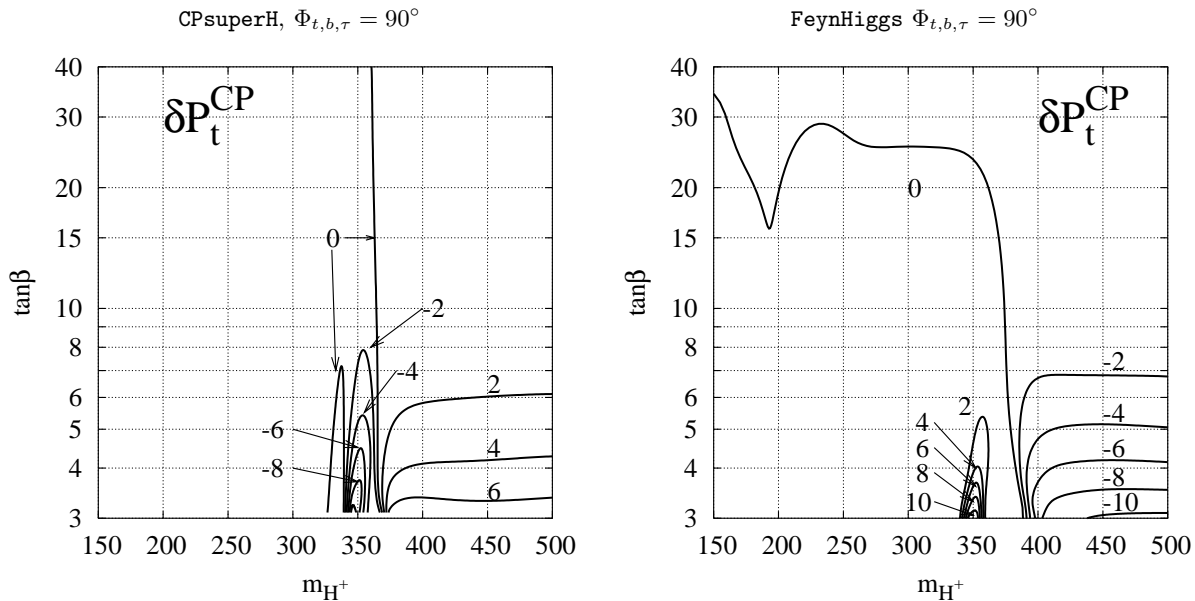


FIG. 7: Contours of constant δP_t^{CP} in units of 10^{-2} in the $(\tan\beta - m_{H^+})$ plane for the CPX scenario with $\Phi_{t,b,\tau} = 90^\circ$ and “peak E_b ” choice. The left panel shows the results obtained with **CPsuperH**, the right panel those obtained with **FeynHiggs**.

Let us now turn to the top polarization in $\gamma\gamma \rightarrow t\bar{t}$. Due to the large top quark mass, here only the heavier Higgs bosons $\phi_{2,3}$ contribute. For the comparatively large m_{H^+} values needed to obtain $m_{\phi_{2,3}} \geq 2m_t$, the mass difference between ϕ_2 and ϕ_3 is usually so small that both their scaled masses can be within the peak of the hard photon spectrum of Fig. 2, although $m_{\phi_3} - m_{\phi_2} \gg \Gamma_{2,3}$ is still maintained. We therefore choose

$$E_b^{\text{peak}} = \max [E_b^0, (m_{\phi_2} + m_{\phi_3}) / (4z_0)], \quad (13)$$

where $E_b^0 = 220$ GeV and $z_0 = 0.8$. Figure 6 shows contours of constant δP_t^\pm in the $(\tan\beta - m_{H^+})$ plane analogous to Fig. 5. Owing to different sign conventions the two programs, δP_t^\pm of **CPsuperH** corresponds to $-\delta P_t^\mp$ in **FeynHiggs**. In Fig. 6 we therefore plot δP_t^- for **CPsuperH** and δP_t^+ for **FeynHiggs**. The deviation from the pure QED prediction (i.e. the Higgs contribution) is sizable for $\tan\beta \lesssim 10$. Note that the CP-even polarization observables for $t\bar{t}$ can reach much larger values than those for $\tau^+\tau^-$. Moreover, in the case of $\gamma\gamma \rightarrow t\bar{t}$ also the CP-odd observable, δP_t^{CP} , may be large enough to be measurable. This is shown in Fig. 7 for $\Phi_{t,b,\tau} = 90^\circ$. Because of the low cross sections, ranging from 8 fb to 150 fb in Fig. 7, as compared to 1–10 pb for the τ case, the statistical fluctuations are large, about $\Delta P_t \sim 0.10 - 0.03$. Therefore the region of sensitivity to the Higgs-boson contributions is restricted to low $\tan\beta$ values.

B. Fixed E_b scan

The “peak E_b ” choice discussed above gives an estimate of the ultimate potential of our polarization observables. In reality, however, one will have a collider running at some fixed beam energy. Obviously it will be of advantage to set E_b such that one is sensitive to the

Higgs contributions over a large part of the parameter space.

In the CPX scenario, **CPsuperH** predicts $m_{\phi_1} \lesssim 123$ GeV. Thus $E_b = 77$ GeV leads to a good sensitivity over most of the parameter space. With **FeynHiggs**, however, the maximum value of m_{ϕ_1} considerably changes with $\Phi_{t,b,\tau}$ in the scan; we obtain maximum values of $m_{\phi_1} = 123$ GeV for $\Phi_{t,b,\tau} = 0^\circ$ and $m_{\phi_1} = 131$ GeV for $\Phi_{t,b,\tau} = 90^\circ$, respectively. Hence we choose $E_b = 77$ GeV for $\Phi_{t,b,\tau} = 0^\circ$ and $E_b = 82$ GeV for $\Phi_{t,b,\tau} = 90^\circ$ in the computation with **FeynHiggs**. The polarization observable δP_τ^- for this fixed E_b choice is shown in the $(\tan\beta - m_{H^+})$ plane in Fig. 8. We observe that for $\Phi_{t,b,\tau} = 90^\circ$, $\delta P_\tau^- \geq 0.01$ unless $\tan\beta$ is very small. For $\Phi_{t,b,\tau} = 0^\circ$, on the other hand, observability of δP_τ^- is limited to $\tan\beta \gtrsim 8-10$. It is apparent that δP_τ will be mainly useful if $\tan\beta$ is large. To explicitly see the phase dependence we show in Fig. 9 contours of constant δP_τ^- in the $(m_{H^+} - \Phi)$ plane for $E_b = 77$ GeV. There is a rather large difference in the results of the two codes, which is also apparent in the other figures, due to differences in the implementation of radiative corrections in the two programs [35]. It is clear that for analyses as suggested in this paper, more precise computations will be necessary.

We next turn to $t\bar{t}$ production with fixed E_b . In this case, as for the peak E_b choice, it is the mean mass of ϕ_2 and ϕ_3 that should be within the peak of the photon spectrum. However, since $m_{\phi_{2,3}}$ change linearly with m_{H^+} , one cannot have optimal sensitivity over the whole parameter space with fixed E_b . We hence take $E_b = 300$ GeV as a good compromise. For this choice one has comparatively large rates while the scaled masses of $\phi_{2,3}$ still lie within the peak of the photon spectrum for a sizable portion of the $(\tan\beta - m_{H^+})$ plane. The results for δP_t^\pm obtained with **CPsuperH** and **FeynHiggs** for $\Phi_{t,b,\tau} = 0^\circ$ and $\Phi_{t,b,\tau} = 90^\circ$ are shown in Fig. 10.

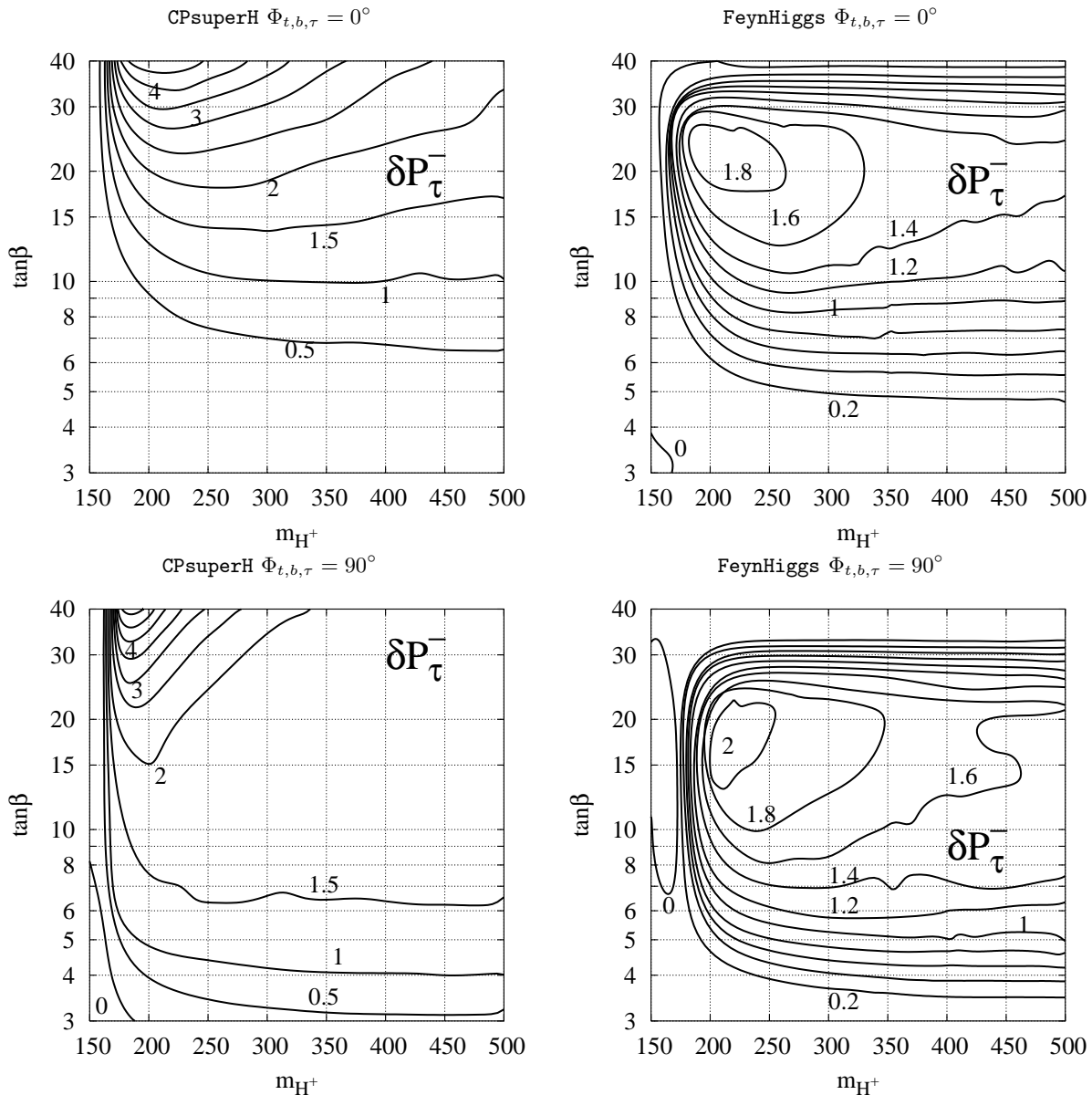


FIG. 8: Contours of constant δP_τ^- in units of 10^{-2} for fixed E_b and $\Phi_{t,b,\tau} = 0^\circ$ and 90° using **CPsuperH** (left panels) and **FeynHiggs** (right panels) to compute the Higgs masses, couplings and widths. $E_b = 77$ GeV, except for the lower-right plot where $E_b = 82$ GeV, see text.

Again the role of δP_t^+ and δP_t^- is interchanged in the two codes. In Fig. 11, we show contours of constant δP_t^{CP} in the $(\Phi - m_{H^+})$ plane for $\tan\beta = 4$ and in Fig. 12 in the $(\Phi - \tan\beta)$ plane for $m_{H^+} = 475$ GeV. As one can see, there is sensitivity to CP violation if $\tan\beta$ is small. Moreover, there is rather good agreement between **CPsuperH** and **FeynHiggs** in δP_t^{CP} (up to a sign). Note also that the signal can be enhanced by tuning E_b .

Comparing these results with the “peak E_b ” choice, we see that for $\gamma\gamma \rightarrow \tau\tau$ one can be sensitive to as large a region of the parameter space if E_b is chosen carefully. For $\gamma\gamma \rightarrow t\bar{t}$, on the other hand, we lose sensitivity to part of the parameter space with fixed E_b .

C. Lepton asymmetries

The polarization of τ leptons can be measured using the energy distribution of the decay pions [22, 36, 37, 38, 39, 40]. The polarization of top quarks can be measured using energy distribution of b quarks [41] or the angular distribution of decay leptons [42, 43, 44, 45]. This kind of analysis requires the full reconstruction of the top momentum. Such a reconstruction may not always be possible for the semi-leptonic decay of the t (or \bar{t}) quark. On the other hand, it is possible to construct simple asymmetries involving the polarization of the initial-state e^\pm (and hence of the photons) and the charge of the final-state lepton, which are sensitive to CP violation. We denote the integrated cross section for the process $\gamma\gamma \rightarrow t\bar{t} \rightarrow l^+\nu b\bar{l} (t\bar{t} \rightarrow \bar{\nu}b)$ by $\sigma(\lambda_{e^-}, Q_I)$, where λ_{e^-}

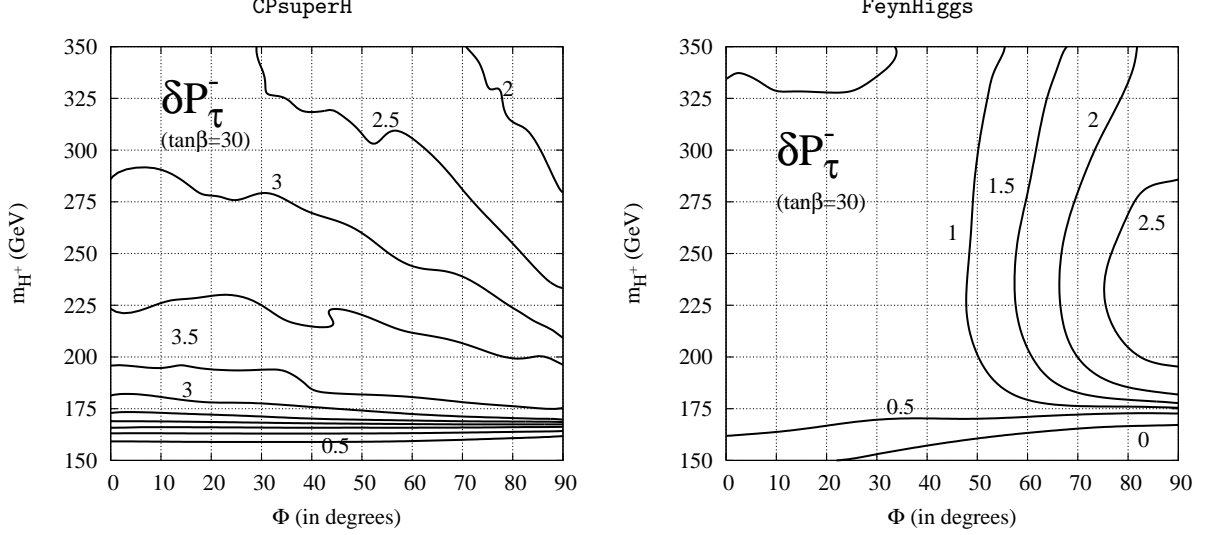


FIG. 9: Contours of constant δP_τ^- in units of 10^{-2} in the $(\Phi_{t,b,\tau} - m_{H^+})$ plane for $\tan\beta = 30$ and $E_b = 77$ GeV with **CPsuperH** (left panel) and **FeynHiggs** (right panel).

is the polarization of the electron beam in the parent collider and Q_l the charge of the secondary lepton coming from the t/\bar{t} decay. The polarizations of all the other beams are adjusted to get a peaked spectrum and equal helicities for the incident photons. With this setup, we can define the following asymmetries [19]:

$$\begin{aligned}
 \mathcal{A}_1 &= \frac{\sigma(+,+) - \sigma(-,-)}{\sigma(+,+) + \sigma(-,-)}, \\
 \mathcal{A}_2 &= \frac{\sigma(+,-) - \sigma(-,+)}{\sigma(+,-) + \sigma(-,+)}, \\
 \mathcal{A}_3 &= \frac{\sigma(+,+) - \sigma(-,+)}{\sigma(+,+) + \sigma(-,+)}, \\
 \mathcal{A}_4 &= \frac{\sigma(+,-) - \sigma(-,-)}{\sigma(+,-) + \sigma(-,-)},
 \end{aligned} \tag{14}$$

Only one of the above asymmetries is independent [19] if no cut is put on the lepton's polar angle in the laboratory frame. Even with a finite cut on the polar angle, the $\mathcal{A}_{1\dots 4}$ have almost identical sensitivities to the Higgs couplings. We use a 20° beam-pipe cut on the lepton. The contours of constant \mathcal{A}_3 for $\Phi_{t,b,\tau} = 30^\circ$ and 90° , using **CPsuperH**, are shown in Fig. 13 for the “peak E_b ” choice. Analogously, Fig. 14 shows \mathcal{A}_3 for fixed $E_b = 300$ GeV and $\Phi_{t,b,\tau} = 30^\circ$ and 90° . The asymmetries are sizable for $\Phi_{t,b,\tau} = 90^\circ$ and decrease rapidly as $\Phi_{t,b,\tau}$ decreases. For $\Phi_{t,b,\tau} = 0^\circ$ the only source of CPV is the phase of M_3 , $\Phi_3 = 90^\circ$, in our scenario. All the y_i 's are then negligibly small as compared to the x_i 's, leading to very small values of the \mathcal{A}_i . Here note that, as shown in Ref. [19], the lepton asymmetries of Eq. (14) are sensitive only to CP-odd combinations of the form factors, i.e. the y_i 's. This should be contrasted with the polarization observables, which are sensitive to both the CP-odd and CP-even combinations.

VI. CONCLUSIONS

We have investigated the use of fermion polarization in the process $\gamma\gamma \rightarrow f\bar{f}$ (with $f = t$ or τ) for studying neutral Higgs bosons at a photon collider. To this aim we have constructed polarization asymmetries δP_f^\pm , which are sensitive to the Higgs exchange contributions. We have also constructed a CP-odd asymmetry δP_f^{CP} which is sensitive to CP violation in the Higgs sector. All these asymmetries are constructed in a model-independent way and can be used to study Higgs bosons in various models beyond the SM.

We have applied this in a numerical analysis to the case of the MSSM with explicit CP violation. In particular we have evaluated our asymmetries for the CPX scenario, using the two public codes **CPsuperH** and **FeynHiggs** to calculate the Higgs masses, couplings and widths.

Scanning the $(\tan\beta - m_{H^+})$ plane for various phases $\Phi_{t,b,\tau}$, we found that δP_τ^\pm is sensitive to a light Higgs, especially if $\tan\beta$ is large. Assuming a measurement accuracy of 10^{-2} for τ polarization, δP_τ^\pm can in fact probe a large part of the CPV-MSSM parameter space. A cut on the $\tau\tau$ invariant mass is, however, necessary to enhance the signal. The CP-odd asymmetry $\delta P_\tau^{\text{CP}}$, on the other hand, is always very small, well below measurability. While δP_τ^\pm can be enhanced by the cut mentioned above, this does not work for $\delta P_\tau^{\text{CP}}$.

This is complemented by the top polarization in $t\bar{t}$ production, which is sensitive to the heavier neutral Higgs bosons $\phi_{2,3}$, and also to CP mixing between them, for $m_{\phi_{2,3}} \geq 2m_t$ and small $\tan\beta$. A similar region is covered by the lepton asymmetries constructed from top decays, which are a pure measure of CP violation. These lepton asymmetries are large for large $\Phi_{t,b,\tau}$ but quickly decrease as this phase decreases.

To conclude, the top and tau polarization asymmetries presented in this paper may prove useful to study the effects of a CP-violating Higgs sector at a photon collider. They may in particular cover the parameter region

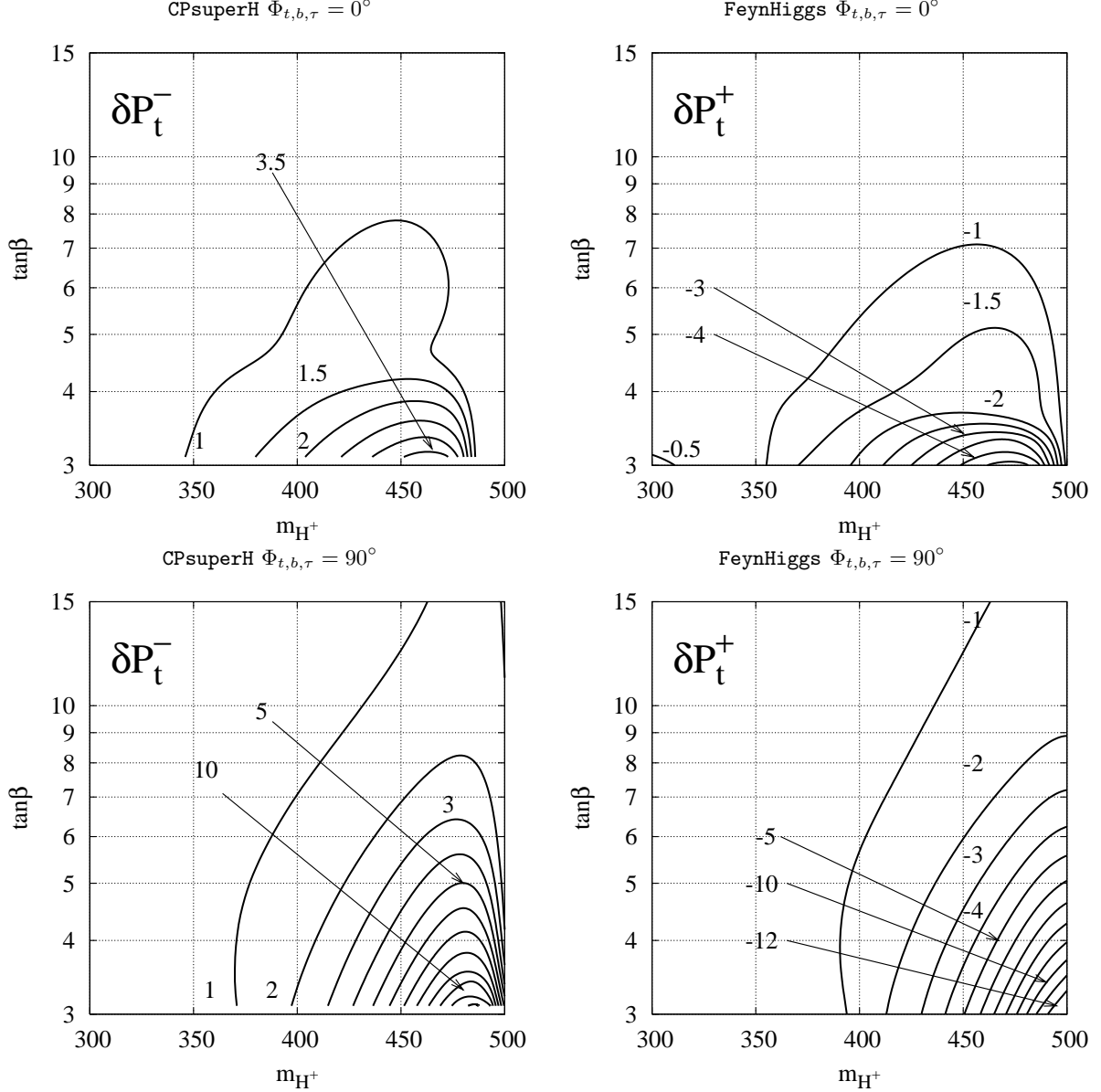


FIG. 10: Contours of constant δP_t^\pm in units of 10^{-2} for fixed $E_b = 300$ GeV and $\Phi_{t,b,\tau} = 0^\circ$ (top) and 90° (bottom) using CPsuperH (left) and FeynHiggs (right) to compute the Higgs masses, couplings and widths.

where a light CP-violating Higgs may have been missed at LEP, and may be missed as well at LHC. We found, however, large quantitative differences between the results obtained with CPsuperH and FeynHiggs. In this regard we emphasize the need for a standardization of these tools.

Note added

While this paper was in preparation, at a point where the numerical analysis was already finished, a new version of FeynHiggs was released, see <http://www.feynhiggs.de> and the contribution on FeynHiggs in [8]. This version contains new radiative corrections also for the CP-violating case. It will be inter-

esting to see their effect on the polarization observables discussed in this paper.

Acknowledgments

We thank S. Heinemeyer for discussions regarding FeynHiggs. R.M.G., S.D.R. and R.K.S. acknowledge the support of the Department of Science and Technology, India, under project no. SP/S2/K-01/2000-II and of the Indo-French Center for the Promotion of Advanced Research under IFCPAR project no. IFC/3004-B/2004. The work of S.K. is financed by an APART (Austrian Program for Advanced Research and Technology) grant of the Austrian Academy of Sciences.

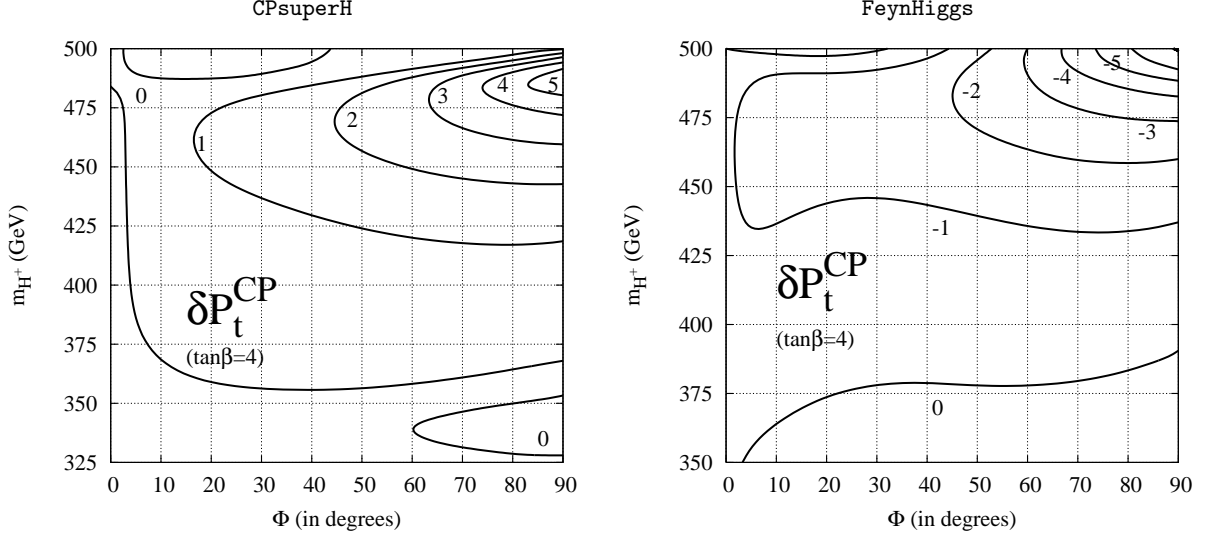


FIG. 11: Contours of constant δP_t^{CP} in units of 10^{-2} in the $(\Phi_{t,b\tau} - m_{H^+})$ plane for $\tan\beta = 4$ and $E_b = 300$ GeV with CPsuperH (left panel) and FeynHiggs (right panel).

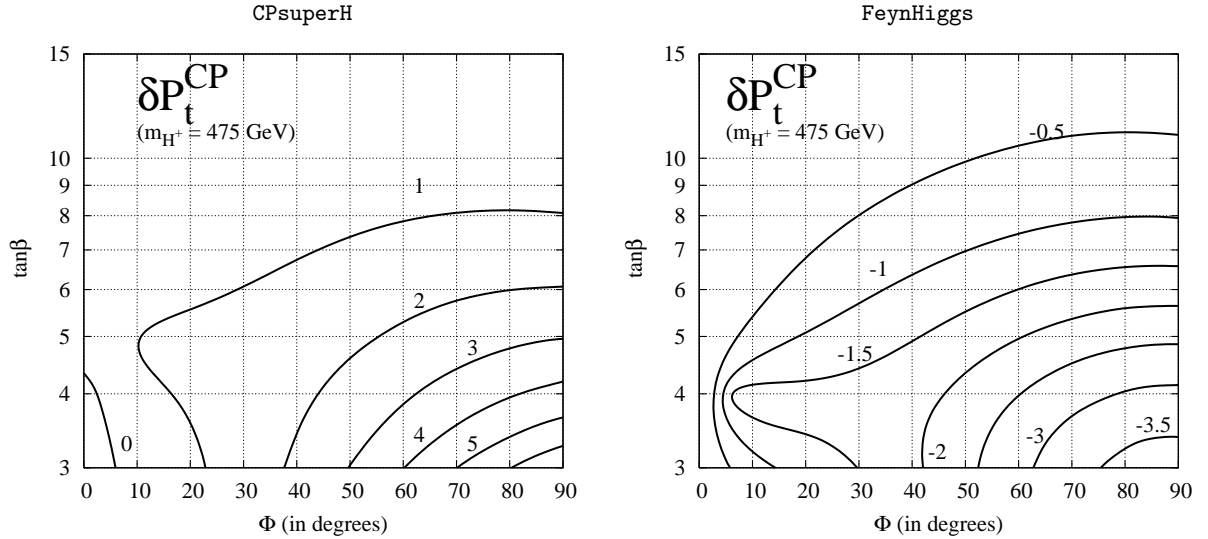


FIG. 12: Contours of constant δP_t^{CP} in units of 10^{-2} in the $(\Phi_{t,b\tau} - \tan\beta)$ plane for $m_{H^+} = 475$ GeV and $E_b = 300$ GeV with CPsuperH (left panel) and FeynHiggs (right panel).

-
- [1] For a review, see for example, R. M. Godbole, hep-ph/0205114, Part A, Volume 4, Jubilee Issue of the Indian Journal of Physics, pp. 44-83, 2004, Guest Editors: A. Raychaudhury and P. Mitra.
- [2] LEP Electroweak Working Group, <http://lepewwg.web.cern.ch/LEPEWWG/>
- [3] ALEPH, DELPHI, L3 and OPAL Collaborations, and the LEP Working Group for Higgs Boson Searches, Phys. Lett. B **565** (2003) 61; see also <http://lephiggs.web.cern.ch/LEPHIGGS/>
- [4] A. Mendez and A. Pomarol, Phys. Lett. B **279** (1992) 98; J. F. Gunion, H. E. Haber and J. Wudka, Phys. Rev. D **43** (1991) 904; J. F. Gunion, B. Grzadkowski, H. E. Haber and J. Kalinowski, Phys. Rev. Lett. **79** (1997) 982; I. F. Ginzburg, M. Krawczyk and P. Osland, hep-ph/0211371.
- [5] ALEPH, DELPHI, L3 and OPAL Collaborations, and the LEP Working Group for Higgs Boson Searches, hep-ex/0602042.
- [6] ATLAS Collaboration, *ATLAS Detector and Physics Performance: Technical Design Report*, vol. 2, CERN-LHCC-99-15 (1999); CMS Collaboration, *CMS physics: Technical Design Report*, vol. 2, CERN-LHCC-2006-021 (2006).
- [7] R.-D. Heuer *et al.*, TESLA TDR-III: Physics at an e^+e^- Linear Collider, hep-ph/0106315; T. Abe *et al.*, Linear Collider Physics Resource Book for Snowmass 2001 - Part 1, hep-ex/0106055; K. Abe *et al.*, ACFA Linear Collider Working Group report, hep-ph/0109166.
- [8] E. Accomando *et al.*, *Workshop on CP studies and non-standard Higgs physics*, CERN-2006-009, hep-ph/0608079.

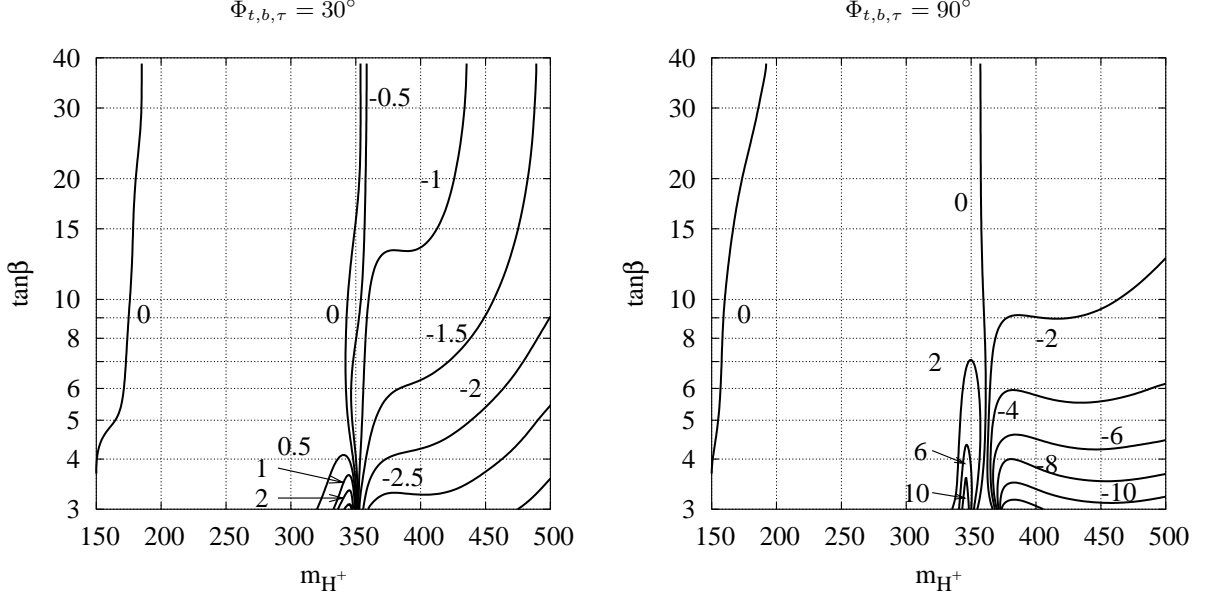


FIG. 13: Contours of constant \mathcal{A}_3 in units of 10^{-2} for “peak E_b ” and $\Phi_{t,b,\tau} = 30^\circ$ and 90° ; Higgs masses, couplings and widths computed with CPsuperH.

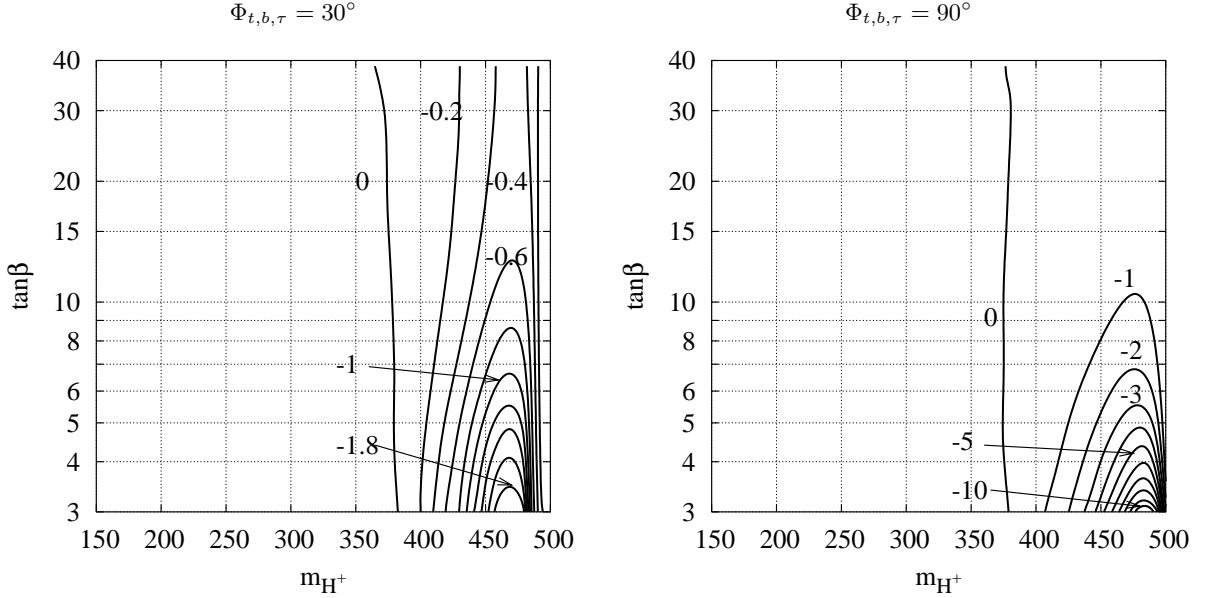


FIG. 14: Contours of constant \mathcal{A}_3 in units of 10^{-2} for fixed $E_b = 300$ GeV and $\Phi_{t,b,\tau} = 30^\circ$ and 90° ; Higgs masses, couplings and widths computed with CPsuperH.

- [9] W. Bernreuther, M. Flesch and P. Haberl, Phys. Rev. D **58** (1998) 114031; W. Bernreuther, A. Brandenburg and M. Flesch, hep-ph/9812387; W. Khater and P. Osland, Nucl. Phys. B **661** (2003) 209.
- [10] J. F. Gunion and X. G. He, Phys. Rev. Lett. **76** (1996) 4468; B. Field, Phys. Rev. D **66** (2002) 114007
- [11] S. Y. Choi, D. J. Miller, M. M. Muhlleitner and P. M. Zerwas, Phys. Lett. B **553** (2003) 61; C. P. Buszello, I. Fleck, P. Marquard and J. J. van der Bij, Eur. Phys. J. C **32**(2004) 209.
- [12] T. Plehn, D. Rainwather, D. Zeppenfeld, Phys. Rev. Lett. **88** (2002) 051801.
- [13] A. Mendez and A. Pomarol, Phys. Lett. B **272** (1991) 313; B. Grzadkowski, J. F. Gunion and J. Kalinowski, Phys. Rev. D **60** (1999) 075011; A. G. Akeroyd and A. Arhrib, Phys. Rev. D **64** (2001) 095018; V. D. Barger, K. M. Cheung, A. Djouadi, B. A. Kniehl and P. M. Zerwas, Phys. Rev. D **49** (1994) 79.
- [14] M. Kramer, J. H. Kuhn, M. L. Stong and P. M. Zerwas, Z. Phys. C **64** (1994) 21; J. F. Gunion, B. Grzadkowski and X. G. He, Phys. Rev. Lett. **77** (1996) 5172; K. Desch, A. Imhof, Z. Was and M. Worek, Phys. Lett. B **579** (2004) 157.
- [15] For a recent summary, see for example, R. M. Godbole, S. Kraml, M. Krawczyk, D. J. Miller, P. Niezurawski and A. F. Zarnecki, hep-ph/0404024.
- [16] B. Badelek *et al.* [ECFA/DESY Photon Collider Working Group Collaboration], “TESLA Technical Design Report, Part VI, Chapter 1: Photon collider at TESLA,” hep-ex/0108012.

- [17] P. Niezurawski, A. F. Zarnecki and M. Krawczyk, JHEP **0211**, 034 (2002); Acta Phys. Polon. B **34** (2003) 177.
- [18] E. Asakawa, S. Y. Choi, K. Hagiwara, J. S. Lee, Phys. Rev. **D62** (2000) 115005
- [19] R. M. Godbole, S. D. Rindani, R. K. Singh, Phys. Rev. **D67** (2003) 095009.
- [20] W.-G. Ma, C.-H. Chang, X.-Q. Li, Z.-H. Yu and L. Han, Commun. Theor. Phys. **26** (1996) 455; Commun. Theor. Phys. **27** (1997) 101.
- [21] K. Hagiwara, A. D. Martin and D. Zeppenfeld, Phys. Lett. **B235** (1990) 198; M. M. Nojiri, Phys. Rev. **D51** (1995) 6281.
- [22] B. K. Bullock, K. Hagiwara and A. D. Martin, Nucl. Phys. B **395** (1993) 499.
- [23] J. R. Ellis, J. S. Lee, A. Pilaftsis, Phys. Rev. D **70** (2004) 075010.
- [24] J. R. Ellis, J. S. Lee and A. Pilaftsis, Nucl. Phys. B **718** (2005) 247.
- [25] J. R. Ellis, J. S. Lee and A. Pilaftsis, Phys. Rev. D **72** (2005) 095006.
- [26] S. Y. Choi, J. Kalinowski, Y. Liao and P. M. Zerwas, Eur. Phys. J. C **40** (2005) 555.
- [27] A. Pilaftsis, Phys. Lett. B **435** (1998) 88; A. Pilaftsis and C. E. M. Wagner, Nucl. Phys. **B553** (1999) 3; D. A. Demir, Phys. Rev. D **60** (1999) 055006; A. Dedes and S. Moretti, Phys. Rev. Lett. **84** (2000) 22, Nucl. Phys. **B576** (2000) 29; S. Y. Choi, M. Drees and J. S. Lee, Phys. Lett. **B481** (2000) 57; M. Carena, J. R. Ellis, S. Mrenna, A. Pilaftsis and C. E. M. Wagner, Nucl. Phys. **B659** (2003) 145.
- [28] M. Carena, J. R. Ellis, A. Pilaftsis and C. E. M. Wagner, Nucl. Phys. **B586** (2000) 92.
- [29] J. S. Lee, A. Pilaftsis, M. Carena, S. Y. Choi, M. Drees, J. R. Ellis, C. E. M. Wagner, Comput.Phys.Comm. **156** (2004) 283.
- [30] S. Heinemeyer, Eur. Phys. J. C **22** (2001) 521.
- [31] I. F. Ginzburg, G. L. Kotkin, S. L. Panfil, V. G. Serbo and V. I. Telnov, Nucl. Instrum. Meth. A **219** (1984) 5.
- [32] A. Pilaftsis, Nucl. Phys. B **504**, 61 (1997).
- [33] E. Asakawa and K. Hagiwara, Eur. Phys. J. **C31** (2003) 351.
- [34] M. Schumacher, in [8]; D.K. Ghosh, R.M. Godbole and D.P. Roy, Phys. Lett. B **628**, 131 (2005).
- [35] See, for instance, S. Heinemeyer, talk at the 1st meeting on *CP studies and non-standard Higgs physics*, 14–15 May 2004, CERN.
- [36] B. K. Bullock, K. Hagiwara and A. D. Martin, Phys. Rev. Lett. **67** (1991) 3055.
- [37] D. P. Roy, Phys. Lett. B **277** (1992) 183.
- [38] S. Raychaudhuri and D. P. Roy, Phys. Rev. D **52** (1995) 1556.
- [39] S. Raychaudhuri and D. P. Roy, Phys. Rev. D **53** (1996) 4902.
- [40] R. M. Godbole, M. Guchait and D. P. Roy, Phys. Lett. B **618** (2005) 193.
- [41] E. Christova and D. Draganov, Phys. Lett. B **434** (1998) 373.
- [42] R. H. Dalitz and G. R. Goldstein, Phys. Rev. D **45** (1992) 1531.
- [43] T. Arens and L. M. Sehgal, Nucl. Phys. B **393** (1993) 46.
- [44] D. Espriu and J. Manzano, Phys. Rev. D **66** (2002) 114009.
- [45] R. M. Godbole, S. D. Rindani and R. K. Singh, arXiv:hep-ph/0605100, To appear in Journal of High Energy Physics (JHEP).